Stochastic solution of a model meson-nucleon field theory

Brian D. Serot
Institute for Theoretical Physics, University of California at Santa Barbara, Santa Barbara, California 93106 and Institute of Theoretical Physics, Department of Physics, Stanford University, Stanford, California 94305

S. E. Koonin
Institute for Theoretical Physics, University of California at Santa Barbara, Santa Barbara, California 93106 and W. K. Kellogg Radiation Laboratory, California Institute of Technology, Pasadena, California 91125

J. W. Negele
Institute for Theoretical Physics, University of California at Santa Barbara, Santa Barbara, California 93106 and Center for Theoretical Physics, Laboratory for Nuclear Science, Massachusetts Institute of Technology, Cambridge, Massachusetts 02139

(Received 20 June 1983)

Ground-state properties in a model quantum field theory are calculated by stochastic evaluation of a path integral representation of the many-body propagator. The model consists of nonrelativistic nucleons coupled to vector and scalar mesons in one spatial dimension. Binding energies and density distributions are calculated for bound states of up to twenty nucleons. The binding energy as a function of density, the nucleon-nucleon correlation function, and the meson-meson correlation function are evaluated in nuclear matter. Exact ground-state solutions to the full field theory are shown to differ relatively little from those of the potential theory corresponding to the static limit. The exact solutions differ substantially from those of the mean-field (Hartree) approximation, but are quite similar to those obtained in the Hartree-Fock approximation.

[NUCLEAR STRUCTURE Meson-nucleon field theory. Monte Carlo solution. Nuclear matter.]

I. INTRODUCTION

A fundamental problem in contemporary nuclear physics is understanding the role of non-nucleon degrees of freedom. The traditional approach to nuclear many-body theory, which has been highly successful, assumes that the physics of the underlying non-nucleon degrees of freedom can be adequately subsumed into a static nucleon-nucleon potential which is then constrained to reproduce two-body observables. In the absence of a tractable theory for the non-nucleon degrees of freedom and definitive experimental constraints, we have at present little understanding of the accuracy of the static-potential approximation or of how the structure of nucleons and their interactions are modified in finite nuclei.

From a theoretical perspective, it is therefore desirable to study a schematic model that includes non-nucleon degrees of freedom and which can be solved exactly. By eliminating uncontrolled approximations to the many-body problem, one can focus directly on the observable differences between the solution to the full theory and the solution to a corresponding static-potential theory in which potentials are defined from exact solution of the two-body problem. At the simplest level, non-nucleon degrees of freedom can be introduced in terms of a field theory in which nucleons interact through their couplings to meson fields; we address such a model field theory in this work. Moreover, studying models containing nucleons and mesons is worthwhile in its own right, as a step toward understanding pion degrees of freedom in nuclear systems. Ultimately, we may be forced to explore the role of quark and gluon degrees of freedom, and, to this extent, the present model should be viewed as a stepping stone towards this goal.

We have two objectives in this work. One is to study a specific model and thereby assess the role of meson dynamics and the accuracy of the static-potential approximation. A second, broader motivation is to develop an approach for studying non-nucleon degrees of freedom which can ultimately be applied to more realistic problems.

The model studied here is constrained by the requirements that it produce nuclear saturation, resulting in nuclei with recognizable liquid-drop behavior, and that it be exactly solvable, thereby avoiding obfuscation from uncontrolled many-body approximations. The first requirement is met by a field theory of the form utilized extensively by Walecka and co-workers[1] containing scalar mesons, which produce the overall binding, and vector mesons, which introduce repulsion at short range. Although, in principle, Monte Carlo techniques can be used to solve such a field theory in any number of spatial dimensions, formidable practical problems associated with fermions arise in more than one dimension, as discussed in

Sec. II. Hence, in the present work we have restricted our attention to a one-dimensional model. For simplicity, rather than necessity, we have also chosen to define the model with nonrelativistic nucleons.

The present model and the Monte Carlo techniques utilized to solve it are subject to significant limitations. Many-body problems in one dimension differ essentially from those in higher dimension, and appropriate care is required in drawing conclusions. The nonrelavistic model precludes an investigation of the effects of the Dirac sea of antinucleons ("baryon vacuum fluctuations") and the importance of relativistic kinematics. The latter is known to play a significant role in the saturation of three-dimensional nuclear systems, as discussed in Ref. 1. We have also omitted internal symmetries and form factors.

The use of Monte Carlo techniques imposes additional limitations. The methods used in this work are restricted to the calculation of ground-state expectation values. Our solutions are exact in the sense that any desired precision can be achieved by increasing the sample size N. In practice, the $N^{-1/2}$ dependence of our statistical errors renders it impractical to compare observables in the full theory and the static-potential theory at a precision substantially higher than one percent. Furthermore, we are currently unable to use the Monte Carlo method to solve the field theory exactly for the scattering of two nucleons. Hence, we cannot test the conventional methodology in which one constrains a phenomenological static potential to reproduce two-body observables.

Having admitted the limitations of the present model, we should also emphasize that many of them can be overcome. The nonrelativistic approximation is inessential, and a relativistic field theory can be treated straightforwardly in one dimension. For the nucleus ^{4}He, the present model is amenable to solution in three spatial dimensions, and the prospects for other systems in higher dimensions will be discussed in subsequent sections. Extensions to simple potential models with quarks, instead of nucleons and mesons, is also possible using, for example, the confining model of Lenz, Moniz, and Yazaki.[2]

The remainder of this paper is organized as follows. In Sec. II, we describe the stochastic method used to evaluate the path integral for the many-body evolution operator. This method is used for the solutions of both the field theory and the many-nucleon problem with static interactions. The model field theory is described in detail in Sec. III. Numerical results are presented and discussed in Sec. IV, and the salient conclusions are contained in the final section. The main text is intended to be self-contained and accessible to a physicist unfamiliar with Monte Carlo methods. Technical details concerning the Monte Carlo calculations are presented in the appendices.

II. METHOD

In this section, we briefly review the method used for finding the exact energy and other ground-state observables of a quantum Hamiltonian system. The basic idea is to evaluate stochastically the imaginary-time Feynman path integral for the many-body evolution operator and hence refine a trial wave function toward the exact wave function. A more detailed exposition, together with simple examples, can be found in Refs. 3–6.

We consider a system with momentum p and conjugate coordinate q whose Hamiltonian is of the form

$$H=T+V \tag{2.1a}$$

$$=\frac{p^2}{2M}+V(q) \tag{2.1b}$$

and seek to determine the energy and other properties of the ground state Ψ_0 of H with energy E_0. For concreteness, one may imagine a single particle moving in one dimension, although the method generalizes simply to many coordinates.

The exact ground state can be obtained by applying the imaginary-time evolution operator to a trial state $\Phi(q)$. The latter is often chosen to have a simple form readily computed analytically. Thus, we define

$$\Psi(t)=\exp\left[\int_0^t E_N(t')dt'\right]e^{-Ht}\Phi\ , \tag{2.2}$$

where $E_N(t')$ is an as yet undetermined, c-number function. Note that as long as $\langle\Psi_0\,|\,\Phi\rangle\neq 0$, $\Psi(t)$ will approach the (unnormalized) exact ground state Ψ_0 as t becomes large.

To compute the exact ground state energy E_0, we consider the quantity

$$E(t)=\frac{\langle\Phi\,|\,H\,|\,\Psi(t)\rangle}{\langle\Phi\,|\,\Psi(t)\rangle} \tag{2.3a}$$

$$=\frac{\int dq\, H\Phi(q)\Psi(q,t)}{\int dq\,\Phi(q)\Psi(q,t)}\ . \tag{2.3b}$$

Clearly, $E(0)$ is the variational energy associated with Φ, $E(t\rightarrow\infty)=E_0$, and $E(t)$ is independent of the function $E_N(t')$. Note that we have used the Hermiticity of H in (2.3b) to express the energy in terms of $H\Phi(q)$, which is presumably a simple function. We now follow Ref. 7 and introduce "importance sampling" by defining

$$G(q,t)=\Phi(q)\Psi(q,t)\ ,$$

so that (2.3b) becomes

$$E(t)=\frac{\int dq\,\epsilon(q)G(q,t)}{\int dq\,G(q,t)}\ . \tag{2.4}$$

That is, the exact energy $E(t)$ is the average of the "local energy"

$$\epsilon(q)=\frac{H\Phi(q)}{\Phi(q)}=-\frac{1}{2M}\frac{1}{\Phi(q)}\frac{\partial^2\Phi(q)}{\partial q^2}+V(q) \tag{2.5}$$

over the distribution $G(q,t)$.

Our evaluation of $E(t)$ is by a Monte Carlo method. Suppose that there exists an ensemble of N "configurations" $\{q_1,\ldots,q_N\}$ distributed according to $G(q,t)$. (We assume here that Φ, Ψ_0, and, hence, G are positive for all q; however, see below.) In this case, an estimate of $E(t)$ is given by

$$E(t)\simeq\frac{1}{N}\sum_{i=1}^{N}\epsilon(q_i)\ . \tag{2.6}$$

Clearly $E(t)$ becomes defined more precisely as N increases. Furthermore, if $\Phi(q)$ is in fact the *exact* solution Ψ_0, then $\epsilon(q)=E_0$, independent of q, and $E(t)=E_0$ with zero variance.

It now remains to specify the algorithm to generate the ensemble of configurations. At $t=0$,

$$G(q,t)=|\Phi(q)|^2 ,$$

so that convenient methods (such as that of Metropolis *et al.*[8]) can be used to generate the initial ensemble, typically having $N\approx$ several hundred members. To evolve the ensemble in time, note that since

$$\partial\Psi/\partial t=(E_N-H)\Psi ,$$

G satisfies the evolution equation

$$\frac{\partial G}{\partial t}=\left[E_N(t)-\Phi(q)H\frac{1}{\Phi(q)}\right]G(q,t) \tag{2.7a}$$

$$=\frac{1}{2M}\frac{\partial^2 G(q,t)}{\partial q^2}-\frac{\partial}{\partial q}[D(q)G(q,t)] -[\epsilon(q)-E_N(t)]G(q,t) . \tag{2.7b}$$

Equation (2.7b) can be interpreted as a diffusion equation for G, with a drift function

$$D(q)=\frac{1}{M}\frac{1}{\Phi(q)}\frac{\partial\Phi(q)}{\partial q} . \tag{2.8}$$

Note that the kinetic energy diffuses G, D tends to keep G confined to regions where Φ is large, and the source "creates" G where $\epsilon(q)$ is smallest. The evolution of G over a short time from t to $t+\Delta t$ can be represented through order Δt by the integral kernel

$$G(q,t+\Delta t)=\int dq' K(q,q';\Delta t)G(q',t) , \tag{2.9a}$$

$$K(q,q';\Delta t)=\exp\{-[\epsilon(q)-E_N(t)]\Delta t\}\exp\left\{\frac{-[q-q'-D(q')\Delta t]^2}{2\Delta t/M}\right\}(M/2\pi\Delta t)^{-1/2} . \tag{2.9b}$$

The algorithm for evolving the ensemble should now be evident. A configuration at time t at the point q' generates a contribution to $G(q,t+\Delta t)$ equal to $K(q,q';\Delta t)$. This is realized by placing in the new ensemble a configuration q distributed as

$$\exp\{-[q-q'-D(q)\Delta t]^2M/2\Delta t\}$$

and then weighting this configuration by

$$\exp\{-[\epsilon(q)-E_N(t)]\Delta t\} .$$

The weighting is effected in practice by replicating or deleting the configuration with probabilities given by this latter function. Thus, N fluctuates from time step to time step but can be held roughly constant by continuous adjustment of E_N. Indeed, to keep $\int dq\, G(q,t)$ (and hence N) constant, $E_N(t)$ should be equal to $E(t)$, so that E_N furnishes a second estimate of $E(t)$, quite independent of that given by (2.6).

In summary, our method is as follows. The system is described by an ensemble of configurations, initially distributed in q according to the trial function $|\Phi(q)|^2$. The overall efficiency of the method is closely related to the accuracy of this trial function. To evolve the ensemble in time, each member is moved in q with a shifted Gaussian probability function [the second factor in Eq. (2.9b)] and then deleted or replicated according to the first factor in Eq. (2.9b). The quantity $E_N(t)$, which is adjusted after each time step to keep the number of configurations in the ensemble roughly constant, provides an estimate of the energy, as does the average $\epsilon(q)$ over the ensemble at any time [Eq. (2.6)]. Furthermore, once the total evolution time is sufficiently large, continued evolution generates independent populations of q distributed according to the exact ground-state wave function, which allows the statistics to be improved to any required accuracy.

Note that since the ensemble moves through configuration space at a rate determined by Δt, which must be sufficiently small so that Eq. (2.9) is accurate, the estimators of the energy will not be independent for successive time steps. Therefore, in forming averages and computing variances of the estimators, care must be taken to collect values only at intervals of t sufficiently large that the values are uncorrelated. Such intervals are conveniently determined by examining the autocorrelation functions of these estimators (see Appendix A).

The evaluation of ground-state expectation values of operators other than the Hamiltonian is complicated because our algorithm readily provides an ensemble representing $G=\Phi\Psi$, rather than one describing $|\Psi|^2$. However, following Ref. 5, if the trial function Φ closely approximates Ψ, then through first order in their difference the expectation value of an Hermitian operator A can be written as

$$\frac{\langle\Psi|A|\Psi\rangle}{\langle\Psi|\Psi\rangle}\simeq 2\frac{\langle\Phi|A|\Psi\rangle}{\langle\Phi|\Psi\rangle}-\frac{\langle\Phi|A|\Phi\rangle}{\langle\Phi|\Phi\rangle} . \tag{2.10}$$

In this case, the second term, which involves the trial function only, is easily evaluated by averaging $A\Phi(q)/\Phi(q)$ over an ensemble distributed according to $|\Phi|^2$, while the first term can be found by averaging $A\Phi(q)/\Phi(q)$ over an ensemble distributed according to $G(q,t)$.

Importance sampling through use of a trial function has been applied successfully to a variety of physical systems, including liquid helium,[9] molecules,[10] the electron gas,[11] liquid and solid hydrogen,[12] and nuclei.[3,13] Whereas the implementation of the algorithm for many-boson systems is straightforward, fermion systems pose special problems,

as discussed in detail in Refs. 3–5, 7, and 11. The requirement of antisymmetry means that Ψ must have nodal surfaces in configuration space. A knowledge of these surfaces is essential in a Monte Carlo method, since the wave function can then be clearly divided into positive and negative regions and each treated separately. In one spatial dimension, antisymmetry alone is sufficient to specify the nodal surface locations, so that simply choosing an antisymmetric Φ is sufficient. (Note that $D(q)$ becomes infinite at a node in $\Phi(q)$ [Eq. (2.8)], as configurations are "repelled" from the nodes.) However, for systems in two or three spatial dimensions, antisymmetry alone is not sufficient to specify the locations of the nodal surfaces; they are determined instead by the dynamics. Several suggestions for dealing with these problems have been put forth. The reader is referred to Refs. 11 and 13 for a detailed discussion.

III. THE MODEL

Our model is inspired by the relativistic quantum field theory of Walecka,[1] which contains nucleons interacting with neutral scalar and vector mesons. Although originally proposed to study high-density matter, this model has recently been shown to provide a reasonable relativistic description of the bulk properties of finite nuclei in the mean-field approximation.[14] However, it is of interest here that for static, heavy baryons, the meson-exchange interaction reduces to a sum of attractive and repulsive Yukawa potentials that can reproduce the basic features of the nucleon-nucleon force. [In one spatial dimension, the Yukawa potentials become exponential potentials; see Eq. (3.17).]

In the following, we will not attempt a systematic nonrelativistic reduction of the Walecka Lagrangian. Instead, this model is used to suggest a simple meson-nucleon field theory containing nonrelativistic nucleons that has a reasonable static-potential limit.

We begin with the covariant Lagrangian density composed of scalar (φ), vector (V_μ), and fermion (ψ) fields:

$$\mathscr{L}=\bar{\psi}(i\gamma_\mu\partial^\mu-M)\psi+\tfrac{1}{2}(\partial_\mu\varphi\partial^\mu\varphi-m_s^2\varphi^2)-\tfrac{1}{4}F^{\mu\nu}F_{\mu\nu}$$
$$+\tfrac{1}{2}m_V^2V_\mu V^\mu-g_V\bar{\psi}\gamma_\mu\psi V^\mu+g_s\bar{\psi}\psi\varphi\ . \tag{3.1}$$

Here

$$F_{\mu\nu}\equiv\partial_\mu V_\nu-\partial_\nu V_\mu\ ,$$

and the conventions used are those of Refs. 14 and 15 with $\hbar=c=1$. In one spatial dimension, scalar products become

$$a_\mu b^\mu=a_0b_0-a_xb_x\ ,$$

and the antisymmetric vector meson field tensor has only one component:

$$F_{0x}=-F_{x0}=\partial V_x/\partial t-\partial V_0/\partial x\ .$$

The two Dirac matrices may be determined as in Chapter 1 of Ref. 15. Denoting the matrices as α and β, one finds $\alpha^2=\beta^2=1$ and $\{\alpha,\beta\}=0$. These relations can be satisfied in a two-dimensional representation, and we choose

$$\gamma^0=\gamma_0=\beta=\sigma_z\ , \tag{3.2}$$

$$\gamma^x=-\gamma_x=\beta\alpha=\sigma_z\sigma_y=-i\sigma_x\ , \tag{3.3}$$

where σ_i are the standard Pauli matrices. The corresponding Dirac spinors also have only two components and so may be interpreted as spinless (i.e., only one positive-energy free-particle solution for a given momentum).

The Hamiltonian density $\mathscr{H}$ can be constructed in the canonical fashion. The Euler-Lagrange equations for the Lagrangian (3.1) consist of three equations of motion:

$$\left[i\beta\frac{\partial}{\partial t}+i\beta\alpha\frac{\partial}{\partial x}-M-g_V\beta V_0+g_V\beta\alpha V+g_s\varphi\right]\psi=0\ , \tag{3.4a}$$

$$\left[\frac{\partial^2}{\partial t^2}-\frac{\partial^2}{\partial x^2}\right]\varphi+m_s^2\varphi=g_s\psi^\dagger\beta\psi\ , \tag{3.4b}$$

$$\frac{\partial}{\partial t}F^{x0}=\frac{\partial E}{\partial t}=m_V^2V-g_V\psi^\dagger\alpha\psi\ , \tag{3.4c}$$

and one equation of constraint:

$$\frac{\partial}{\partial x}F^{x0}=\frac{\partial E}{\partial x}=-m_V^2V_0+g_V\psi^\dagger\psi\ . \tag{3.5}$$

Here we define the "electric field" $E\equiv F^{x0}=-F^{0x}$ and omit the spatial index on field variables; that is, $V\equiv V^x$. The momenta conjugate to the fields are the following:

$$\pi_F=\frac{\delta\mathscr{L}}{\delta(\partial\psi/\partial t)}=i\psi^\dagger\ , \tag{3.6a}$$

$$\pi_s=\frac{\delta\mathscr{L}}{\delta(\partial\varphi/\partial t)}=\frac{\partial\varphi}{\partial t}\ , \tag{3.6b}$$

$$\pi_V=\frac{\delta\mathscr{L}}{\delta(\partial V/\partial t)}=\frac{\partial V}{\partial t}+\frac{\partial V_0}{\partial x}=-E\ , \tag{3.6c}$$

$$\pi_0=\frac{\delta\mathscr{L}}{\delta(\partial V_0/\partial t)}=0\ . \tag{3.6d}$$

Since the timelike component V_0 has no conjugate momentum, it is not a dynamical variable and many be eliminated in favor of $\partial E/\partial x$ using Eq. (3.5). The equations of motion for the electric field and vector field are then Eq. (3.4c) and

$$\frac{\partial V}{\partial t}=-E+\frac{1}{m_V^2}\frac{\partial^2E}{\partial x^2}-\frac{g_V}{m_V^2}\frac{\partial}{\partial x}(\psi^\dagger\psi)\ . \tag{3.7}$$

The Hamiltonian density is given by

$$\mathscr{H}=\sum_{\text{fields}}\pi\frac{\partial\varphi}{\partial t}-\mathscr{L} \tag{3.8a}$$

$$\equiv\mathscr{H}_F^0+\mathscr{H}_s^0+\mathscr{H}_V^0+\mathscr{H}_{\text{int}}\ , \tag{3.8b}$$

with the result

$$\mathscr{H}_F^0=\psi^\dagger\left[-i\alpha\frac{\partial}{\partial x}+\beta M\right]\psi\ , \tag{3.9a}$$

$$\mathscr{H}_s^0=\tfrac{1}{2}\left[\pi_s^2+\left[\frac{\partial\varphi}{\partial x}\right]^2+m_s^2\varphi^2\right], \tag{3.9b}$$

$$\mathscr{H}_V^0=\tfrac{1}{2}\left[E^2+\frac{1}{m_V^2}\left[\frac{\partial E}{\partial x}\right]^2+m_V^2V^2\right], \tag{3.9c}$$

$$\mathscr{H}_{\rm int}=\psi^\dagger\left[-g_V\alpha V-\frac{g_V}{m_V^2}\left[\frac{\partial E}{\partial x}\right]-g_s\beta\varphi\right]\psi + \frac{1}{2}\frac{g_V^2}{m_V^2}(\psi^\dagger\psi)(\psi^\dagger\psi)\,. \tag{3.9d}$$

Note that all factors of V_0 have been eliminated using Eq. (3.5) to express $\mathscr{H}$ solely in terms of dynamical variables. There is also a density-density contact interaction between nucleons [the last term in (3.9d)] analogous to the Coulomb interaction in QED.

To this point, all manipulations have been carried out in a relativistic framework. We now define our nonrelativistic (NR) model in the following fashion. First, we neglect all contributions from antinucleons and from the lower ("small") components of the Dirac spinors. This allows the two-component Dirac fields ψ to be replaced with one-component Schrödinger fields $\psi_{\rm NR}$. Second, we replace Eq. (3.9a) with the Schrödinger Hamiltonian

$$\mathscr{H}_F^0\to\psi_{\rm NR}^\dagger\left[M+\frac{p^2}{2M}\right]\psi_{\rm NR} \tag{3.10}$$

with $p=-i\partial/\partial x$. Finally, we neglect the coupling between the vector field and the baryon current density: $-g_V\psi^\dagger\alpha\psi V$. Since $\alpha=\sigma_y$ is an odd matrix, $\psi^\dagger\alpha\psi$ involves products of upper and lower Dirac components, and this coupling is a correction of order $(1/M)$ compared to the terms retained. This final approximation is not essential, but greatly simplifies the subsequent numerical work. (See the discussion in Appendix B.)

With the preceding simplifications, the model Hamiltonian for the meson-nucleon system is

$$H=\int dx\,\mathscr{H}(x)$$

$$=\sum_{i=1}^{A}\frac{p_i^2}{2M}+\tfrac{1}{2}\int dx\left[\pi_s^2+\left[\frac{\partial\varphi}{\partial x}\right]^2+m_s^2\varphi^2\right]+\tfrac{1}{2}\int dx\left[E^2+\frac{1}{m_V^2}\left[\frac{\partial E}{\partial x}\right]^2+m_V^2V^2\right]$$

$$-g_s\int dx\,\varphi(x)\rho(x)-\frac{g_V}{m_V^2}\int dx\left[\frac{\partial E}{\partial x}\right]\rho(x)+\frac{1}{2}\frac{g_V^2}{m_V^2}\int dx\,\rho(x)\rho(x) \tag{3.11a}$$

$$=\sum_{i=1}^{A}\frac{p_i^2}{2M}+\tfrac{1}{2}\int dx\left[\pi_s^2+\left[\frac{\partial\varphi}{\partial x}\right]^2+m_s^2\varphi^2\right]+\tfrac{1}{2}\int dx\left[E^2+\frac{1}{m_V^2}\left[\frac{\partial E}{\partial x}\right]^2+m_V^2V^2\right]$$

$$-g_s\sum_{i=1}^{A}\varphi(x_i)-\frac{g_V}{m_V^2}\sum_{i=1}^{A}\left[\frac{\partial E}{\partial x}\right]_{x=x_i}+\frac{1}{2}\frac{g_V^2}{m_V^2}\sum_{i,j=1}^{A}\delta(x_i-x_j)\,. \tag{3.11b}$$

Here we have returned to first-quantized coordinates x_i and momenta p_i for A nucleons and have dropped the constant contribution from the nucleon mass. The baryon density has the first-quantized form

$$\psi_{\rm NR}^\dagger(x)\psi_{\rm NR}(x)=\rho(x)=\sum_{i=1}^{A}\delta(x-x_i)\,. \tag{3.12}$$

Note that we have only one type of fermion, i.e., no spin or isospin degrees of freedom.

The preceding Hamiltonian contains M, m_s, g_s, m_V, and g_V as parameters. Since M appears only in the nucleon kinetic energy, we fix the nucleon mass at its physical value: $M=939$ MeV. The remaining constants can be fixed, in principle, by calculating some small set of observables (binding energies, saturation density, etc.) as functions of the parameters and then using physical values to specify g_s, m_s, g_V, and m_V. Since we are interested primarily in the qualitative features of the model, we follow the simpler approach described below.

First, we consider nuclear matter confined in a large box of length L at nucleon density

$$\rho=\int_{-k_F}^{k_F}\frac{dk}{2\pi}=\frac{k_F}{\pi} \tag{3.13}$$

and solve for the ground-state energy in the mean-field (MF) approximation. By translational invariance in space and time, all derivatives of the (c-number) meson fields vanish, as does the spatial component V. The total binding-energy density then follows from (3.11):

$$\frac{E_{\rm MF}}{L}=\mathscr{E}_{\rm MF}=\frac{\pi^2}{6}\frac{\rho^3}{M}+\tfrac{1}{2}m_s^2\varphi_0^2-g_s\varphi_0\rho+\frac{1}{2}\frac{g_V^2}{m_V^2}\rho^2\,. \tag{3.14}$$

The first term is the nucleon kinetic energy, and we may eliminate the mean scalar field φ_0 by solving (3.4b) in the nonrelativistic limit[16]: $\varphi_0=g_s\rho/m_s^2$. Dividing Eq. (3.14) by the baryon density gives the binding energy per nucleon:

$$\frac{E_{\rm MF}}{A}=\frac{\pi^2}{6}\frac{\rho^2}{M}+\frac{1}{2}\left[\frac{g_v^2}{m_v^2}-\frac{g_s^2}{m_s^2}\right]\rho\,. \tag{3.15}$$

The saturation density ρ_0 is determined by

$$[\partial(E_{\rm MF}/A)/\partial\rho]_{\rho_0}=0\,.$$

We fix the binding energy at saturation to be

TABLE I. Model parameters.

$g_s=196$ MeV	$m_s=140$ MeV
$g_V=890$ MeV	$m_V=783$ MeV
$\hbar^2/M=41.467$ MeV fm^2	

$$(E_{\rm MF}/A)_{\rho_0}=-\alpha_1=-16 \text{ MeV} ,$$

motivated by three-dimensional nuclear matter. Note that in the mean-field approximation, specifying the binding energy determines the saturation density. Thus, the two saturation conditions may be solved for ρ_0 and for the combination of parameters appearing in (3.15). We find

$$\zeta\equiv\frac{g_V^2}{m_V^2}-\frac{g_s^2}{m_s^2}=-\pi\left[\frac{8a_1}{3M}\right]^{1/2}=-0.670 , \tag{3.16a}$$

$$\rho_0=0.484 \text{ fm}^{-1} . \tag{3.16b}$$

This procedure imposes only one constraint on the four free parameters. To specify them uniquely, we consider the static potential resulting from scalar and vector meson exchange. In one spatial dimension, this is given by

$$U(x)=\frac{1}{2}\left[\frac{g_V^2}{m_V}e^{-m_V|x|}-\frac{g_s^2}{m_s}e^{-m_s|x|}\right] . \tag{3.17}$$

Our one-dimensional system saturates in the mean-field approximation as long as the volume integral of $U(x)$,

$$\int_{-\infty}^{\infty} dx\, U(x)=\zeta ,$$

is attractive ($\zeta<0$). To arrive at a reasonable nucleon-nucleon potential, we demand that it have a repulsive core [$U(x=0)>0$] and that it have a sensible core radius [defined by $U(x=x_c)=0$], which we fix to be $x_c=0.4$ fm. Finally, the potential will have a sensible range if the meson masses are approximately several hundred MeV. We therefore choose $m_s=m_\pi=140$ MeV and $m_V=m_\omega=783$ MeV as representative values. These considerations are sufficient to specify the four parameters and lead to the values in Table I. The resulting static potential is shown in Fig. 1.

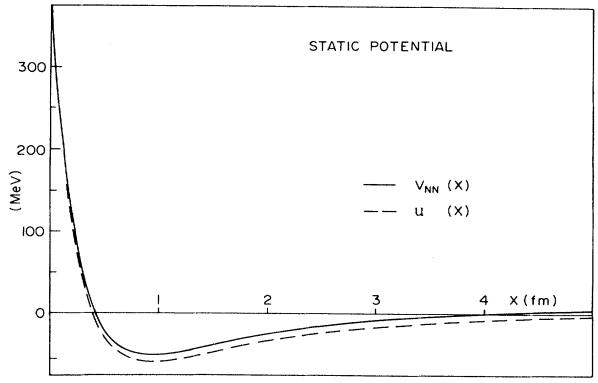

FIG. 1. Static potentials for the nuclear model. The dashed curve denotes the sum over exponentials $U(x)$ [Eq. (3.17)] obtained in the static limit for an infinite domain. The solid curve indicates the interaction $V_{\rm NN}(x)$ [Eq. (3.35)] on the periodic lattice of length 16 fm with the $n=0$ mode removed.

Having completely specified the model, we proceed to cast our Hamiltonian into a form suitable for Monte Carlo calculations of ground-state properties. In practice (see Sec. II), the ground-state wave function is represented by an ensemble of configurations. The nucleons in each configuration are described by their spatial coordinates $\{x_i\}$. However, since the mesons are represented by quantum fields, their description requires (in principle) an infinite set of coordinates. One possible solution to this problem is to define a spatial mesh and to specify the fields by their values at each mesh point. However, to retain a continuous variation of nucleon coordinates, we have chosen instead to apply periodic boundary conditions (i.e., put the system on a "ring") and to describe the meson fields by their Fourier components. This description is also useful because it allows us to "freeze out" the high-energy field components, whose dynamics are unimportant at nuclear energy scales, as we discuss below.

If the system is periodic with length L, the baryon density and scalar field can be decomposed as

$$\rho(x)=\sum_{i=1}^{A}\delta(x-x_i)$$

$$=\sqrt{2/L}\left\{\tfrac{1}{2}\rho_0+\sum_{n=1}^{\infty}\left[\rho_n\sin\left[\frac{2\pi n}{L}x\right]+\tilde{\rho}_n\cos\left[\frac{2\pi n}{L}x\right]\right]\right\} , \tag{3.18}$$

$$\varphi(x)=\sqrt{2/L}\left\{\tfrac{1}{2}\varphi_0+\sum_{n=1}^{\infty}\left[\varphi_n\sin\left[\frac{2\pi n}{L}x\right]+\tilde{\varphi}_n\cos\left[\frac{2\pi n}{L}x\right]\right]\right\} , \tag{3.19}$$

and similarly for $E(x)$. Since $(-E(x))$ and $V(x)$ are conjugate variables [cf. Eq. (3.6c)], we are free to choose $(-E(x)/m_V)$ as the field coordinate and $(m_V V(x))$ as the momentum. This is clearly advantageous from the form of the Hamiltonian in Eq. (3.11), as now the nucleon coordinates couple only to the fields and not their momenta. The conjugate field momentum operators follow immediately from Eq. (3.19):

$$\pi_s(x)=-i\frac{\delta}{\delta\varphi(x)}=-i\sum_n\frac{\delta\varphi_n}{\delta\varphi(x)}\frac{\partial}{\partial\varphi_n}$$
$$=-i\sqrt{2/L}\left\{\frac{\partial}{\partial\varphi_0}+\sum_{n=1}^{\infty}\left[\sin\left[\frac{2\pi n}{L}x\right]\frac{\partial}{\partial\varphi_n}+\cos\left[\frac{2\pi n}{L}x\right]\frac{\partial}{\partial\tilde{\varphi}_n}\right]\right\} \tag{3.20}$$

and similarly for $m_V V(x)$.

Substitution of the Fourier decompositions into Eq. (3.11) yields the Hamiltonian operator

$$H=-\frac{1}{2M}\sum_{i=1}^{A}\frac{\partial^2}{\partial x_i^2}-\tfrac{1}{2}\sum_{n=1}^{\infty}\left[\frac{\partial^2}{\partial\varphi_n^2}-\omega_n^2\varphi_n^2+\frac{\partial^2}{\partial\hat{E}_n^2}-\Omega_n^2\hat{E}_n^2\right]$$
$$-g_s\sum_{n=1}^{\infty}\varphi_n\rho_n-\frac{g_V}{m_V}\sum_{i=1}^{A}\sum_{n=1}^{\infty}\hat{E}_n\frac{\partial\rho_n}{\partial x_i}+\frac{1}{2}\frac{g_V^2}{m_V^2}\sum_{n=1}^{\infty}\rho_n^2+H_0-E_{\rm vac}\ , \tag{3.21}$$

where

$$\omega_n\equiv\left[\left[\frac{2\pi n}{L}\right]^2+m_s^2\right]^{1/2}, \tag{3.22a}$$

$$\Omega_n\equiv\left[\left[\frac{2\pi n}{L}\right]^2+m_V^2\right]^{1/2}, \tag{3.22b}$$

$$\hat{E}\equiv E_n/m_V\ . \tag{3.22c}$$

Here and henceforth we indicate explicitly the Fourier sums over sine components only, since the sums over cosine components $\tilde{\varphi}_n$, $\tilde{\rho}_n$, etc., have identical form. The coupling between the nucleons and the electric field has been rewritten by inverting the Fourier transform of the density, resulting in

$$\rho_0=\sqrt{2/L}\,A\ , \tag{3.23a}$$

$$\rho_n=\sqrt{2/L}\sum_{i=1}^{A}\sin\left[\frac{2\pi n}{L}x_i\right], \tag{3.23b}$$

$$\tilde{\rho}_n=\sqrt{2/L}\sum_{i=1}^{A}\cos\left[\frac{2\pi n}{L}x_i\right], \tag{3.23c}$$

$$\rho(x)=\frac{A}{L}+\frac{2}{L}\sum_{i=1}^{A}\sum_{n=1}^{\infty}\left[\sin\left[\frac{2\pi n}{L}x_i\right]\sin\left[\frac{2\pi n}{L}x\right]+\cos\left[\frac{2\pi n}{L}x_i\right]\cos\left[\frac{2\pi n}{L}x\right]\right]. \tag{3.23d}$$

We have also subtracted from H the infinite vacuum (zero-point) energy for the fields

$$E_{\rm vac}=\tfrac{1}{2}\sum_{n=1}^{\infty}(\omega_n+\Omega_n)\ , \tag{3.24}$$

which is a physically irrelevant constant.

We consider now the Hamiltonian H_0 involving the $n=0$ modes:

$$H_0=-\frac{\partial^2}{\partial\varphi_0^2}+\tfrac{1}{4}m_s^2\varphi_0^2-\frac{g_s}{\sqrt{2L}}\varphi_0 A-\frac{\partial^2}{\partial\hat{E}_0^2}$$
$$+\tfrac{1}{4}m_V^2\hat{E}_0^2+\frac{1}{2}\frac{g_V^2}{m_V^2}\frac{A^2}{L}-\tfrac{1}{2}(m_s+m_V)\ . \tag{3.25}$$

This term decouples from the remaining Hamiltonian and can be solved exactly, since it is of simple-harmonic-oscillator form. We find

$$E_0(A)=\frac{1}{2}\left[\frac{g_V^2}{m_V^2}-\frac{g_s^2}{m_s^2}\right]\frac{A^2}{L}\ . \tag{3.26}$$

Note that E_0 is completely determined by A and L, and vanishes as $L\to\infty$ for a finite system. In infinite nuclear matter, the $n=0$ mode energy per nucleon is precisely the mean-field interaction energy [cf. Eq. (3.15)]. This is correct, since the mean field approximation retains only the volume integral of the static potential (that is, the $n=0$ modes).

Since E_0 is a well-defined constant, it can be omitted from the Monte Carlo algorithm and explicitly included later. In particular, E_0 depends explicitly on L, and binding energies are defined relative to infinitely separated nucleons, so it is necessary to include E_0 in the calculation of the binding energy. An alternative way to see this is to consider ordinary potential theory. Omission of the $n=0$ modes corresponds to shifting the definition of the potential energy by an L-dependent constant. Although the shift goes to zero as $1/L$, omitting E_0 for $L=16$ fm yields an error of 45 MeV in the saturation energy per nucleon in nuclear matter. If we explicitly include the $n=0$ modes, the binding energy E_B can be calculated from

$$-E_B=\hat{E}(A)+E_0(A)-A[\hat{E}(1)+E_0(A=1)]$$
$$=\hat{E}(A)-A\hat{E}(1)+(A^2-A)E_0(A=1)\ , \tag{3.27}$$

where $E_0(A)$ is given by Eq. (3.26), and $\hat{E}(A)$ denotes the energy of A nucleons in a box of length L ignoring the $n=0$ modes.

After subtracting the vacuum energy (3.24) and E_0, the Hamiltonian can be written as

$$H=-\frac{1}{2M}\sum_{i=1}^{A}\frac{\partial^2}{\partial x_i^2}-\tfrac{1}{2}\sum_{n=1}^{\infty}\left[\frac{\partial^2}{\partial\varphi_n^2}-\omega_n^2\varphi_n^2+\frac{\partial^2}{\partial\hat{E}_n^2}-\Omega_n^2\hat{E}_n^2\right]$$
$$-g_s\sum_{n=1}^{\infty}\varphi_n\rho_n-\frac{g_V}{m_V}\sum_{i=1}^{A}\sum_{n=1}^{\infty}\hat{E}_n\frac{\partial\rho_n}{\partial x_i}+\frac{1}{2}\frac{g_V^2}{m_V^2}\sum_{n=1}^{\infty}\rho_n^2-\tfrac{1}{2}\sum_{n=1}^{\infty}(\omega_n+\Omega_n)\,, \tag{3.28}$$

where ρ_n is defined by Eqs. (3.23), and the Fourier sums run over both sine and cosine components. This Hamiltonian is of the general form described in Sec. II, involving coordinates x_i, $\hat{E}_n$, and φ_n, momenta $\partial/\partial x_i$, $\partial/\partial\varphi_n$, and $\partial/\partial\hat{E}_n$, and couplings between the various coordinates. Nevertheless, there is still an infinite number of mesonic degrees of freedom, and Eq. (3.28) is intractable as it stands. To reduce the coordinates to a finite number, we consider H in the static limit, which is obtained formally by letting $M\to\infty$. This eliminates the nucleon kinetic energy and results in fixed nucleon coordinates $\{x_i\}$; consequently, the Fourier components of the density ρ_n are constant as well. In this limit, the vector and scalar fields are independent, and the resulting Hamiltonian is of the form of shifted harmonic oscillators in the field variables. It may be solved exactly for the (unnormalized) ground-state meson wave function:

$$\Phi_0(\varphi_n,\hat{E}_n)=\prod_{n=1}^{\infty}\exp[-\tfrac{1}{2}\omega_n(\varphi_n-\chi_n)^2$$
$$-\tfrac{1}{2}\Omega_n(\hat{E}_n-\zeta_n)^2]\,, \tag{3.29}$$

where

$$\chi_n=\frac{1}{\omega_n^2}g_s\rho_n\,, \tag{3.30a}$$

$$\xi_n=\frac{1}{\Omega_n^2}\frac{g_V}{m_V}\sum_{i=1}^{A}\frac{\partial\rho_n}{\partial x_i}\,. \tag{3.30b}$$

The energy is given in this limit by

$$E_{\text{static}}=-\tfrac{1}{2}g_s^2\sum_{n=1}^{\infty}\frac{\rho_n^2}{\omega_n^2}+\tfrac{1}{2}g_V^2\sum_{n=1}^{\infty}\frac{\rho_n^2}{\Omega_n^2}+E_0 \tag{3.31}$$

with ρ_n the Fourier components of the static nucleon density.

The static limit is useful because nuclear energy scales are significantly smaller than the meson masses. Thus the dynamics of the high-frequency meson modes will be unimportant for the nuclear systems studied here. It is therefore possible to "freeze out" these modes by replacing this part of the true meson wave function with the static result in Eq. (3.29). We then consider a finite number n_s of dynamic scalar modes and n_V vector modes. In principle, the cutoffs n_s and n_V can be increased until convergence is reached; we expect, however, that for momenta $(2\pi n/L)\gtrsim M$, the static approximation should be reasonable.

To replace the high-frequency meson modes with their static counterparts, we first calculate the energy of a single, fixed nucleon ($\rho_n^2+\tilde{\rho}_n^2=2/L$) using Eq. (3.31):

$$E_1=-\frac{1}{L}g_s^2\sum_{n=1}^{\infty}\frac{1}{\omega_n^2}+\frac{1}{L}g_v^2\sum_{n=1}^{\infty}\frac{1}{\Omega_n^2}\,. \tag{3.32}$$

[The static $n=0$ mode energy $E_0(1)$ can again be treated separately.] Using the identity

$$S_\alpha(x)\equiv\sum_{n=-\infty}^{\infty}\frac{\cos(2\pi nx/L)}{n^2+a_\alpha^2}$$
$$=\frac{2\pi^2}{m_\alpha L}\frac{\cosh[m_\alpha(L/2-|x|)]}{\sinh(m_\alpha L/2)} \tag{3.33}$$

with $a_\alpha\equiv m_\alpha L/2\pi$, we find

$$E_1=-\frac{g_s^2L}{8\pi^2}\left[S_s(0)-\frac{1}{a_s^2}\right]$$
$$+\frac{g_V^2L}{8\pi^2}\left[S_V(0)-\frac{1}{a_V^2}\right]\,. \tag{3.34}$$

Consider now two fixed nucleons separated by a distance x, for which

$$\rho_n^2+\tilde{\rho}_n^2=\frac{2}{L}[2+2\cos(2\pi nx/L)]\,.$$

The static energy may again be calculated from Eqs. (3.31) and (3.33), and the two-nucleon potential defined as the difference between this energy and $2E_1$. We find

$$V_{\text{NN}}(x)=\frac{-g_s^2L}{4\pi^2}\left[S_s(x)-\frac{1}{a_s^2}\right]$$
$$+\frac{g_V^2L}{4\pi^2}\left[S_V(x)-\frac{1}{a_V^2}\right]\,, \tag{3.35}$$

which is plotted in Fig. 1 for the parameters given in Table I and $L=16$ fm. $V_{\text{NN}}(x)$ explicitly incorporates the periodic nature of the meson fields and omits the $n=0$ mode contribution, which is a spatial (but L-dependent) constant. Note also that Eqs. (3.34) and (3.35) imply that the static, single-nucleon self-energy is given by $E_1=\frac{1}{2}V_{\text{NN}}(0)$.

Having defined the two-nucleon potential for the periodic system, we construct the Hamiltonian as follows. Begin with A nucleons interacting through $V_{\text{NN}}(x)$:

$$H_{\text{static}}=-\frac{1}{2M}\sum_{i=1}^{A}\frac{\partial^2}{\partial x_i^2}+\frac{A}{2}V_{\text{NN}}(0)$$
$$+\sum_{i<j=1}^{A}V_{\text{NN}}(x_i-x_j)\,. \tag{3.36}$$

Here the second term gives the total nucleon self-energy, and, at this stage, all meson modes are "frozen out." To incorporate a finite number of dynamic modes, we *remove* their static energy using Eq. (3.31) and *replace* it with the dynamic expression in Eq. (3.28). Thus, the desired Hamiltonian is written as

$$H=-\frac{1}{2M}\sum_{i=1}^{A}\frac{\partial^2}{\partial x_i^2}+\frac{A}{2}V_{\mathrm{NN}}(0)+\sum_{i<j=1}^{A}V_{\mathrm{NN}}(x_i-x_j)$$
$$-\left[-\tfrac{1}{2}g_s^2\sum_{n=1}^{n_s}\frac{\rho_n^2}{\omega_n^2}+\tfrac{1}{2}g_V^2\sum_{n=1}^{n_V}\frac{\rho_n^2}{\Omega_n^2}\right]-\tfrac{1}{2}\sum_{n=1}^{n_s}\left[\frac{\partial^2}{\partial\varphi_n^2}-\omega_n^2\varphi_n^2\right]$$
$$-\tfrac{1}{2}\sum_{n=1}^{n_V}\left[\frac{\partial^2}{\partial\hat{E}_n^2}-\Omega_n^2\hat{E}_n^2\right]-g_s\sum_{n=1}^{n_s}\varphi_n\rho_n-\frac{g_V}{m_V}\sum_{i=1}^{A}\sum_{n=1}^{n_V}\hat{E}_n\frac{\partial\rho_n}{\partial x_i}$$
$$+\frac{1}{2}\frac{g_V^2}{m_V^2}\sum_{n=1}^{n_V}\rho_n^2-\tfrac{1}{2}\sum_{n=1}^{n_s}\omega_n-\tfrac{1}{2}\sum_{n=1}^{n_V}\Omega_n\ . \tag{3.37}$$

The static limit is obtained by setting $n_s=n_V=0$. The omitted $n=0$ mode energy is included in the calculation of binding energies using Eq. (3.27), where $\hat{E}(A)$ is calculated with Eq. (3.37). We emphasize that had we simply truncated the sums in Eq. (3.28) and not replaced the high-frequency modes by their static limits, many more meson modes would be needed to describe the interaction accurately.

The preceding Hamiltonian is of the form studied in Sec. II and contains a finite number of degrees of freedom. To implement the "importance sampling," we need only specify a suitable trial wave function. We take

$$\Phi(x_i,\varphi_n,\hat{E}_n)=\Lambda(\{x_i\})\prod_{n=1}^{n_s}e^{-(1/2)\omega_n[\varphi_n-\chi_n(x)]^2}\times\prod_{m=1}^{n_V}e^{(-1/2)\Omega_m[\hat{E}_m-\xi_m(x)]^2}\ . \tag{3.38}$$

The meson part is similar to the static solution (3.29). Here, however, the functions $\chi_n(x)$ and $\xi_n(x)$ are calculated from Eq. (3.30) for a given set of nucleon coordinates, whose distribution is specified by $\Lambda(\{x_i\})$. The trial wave function Φ constitutes a type of Born-Oppenheimer approximation in which the dynamic part of the meson wave function is determined by the instantaneous nucleon coordinates. Our choice of Λ is discussed in the following section.

IV. RESULTS

Monte Carlo calculations were performed for ground state observables of finite nuclei and nuclear matter. To understand the role of dynamic mesons, calculations in the static-potential limit, with all meson modes frozen, were compared with corresponding results with dynamic meson modes.

As discussed in the previous section, calculations with dynamic mesons require a truncation in the number of modes appearing in the Fourier expansion of the fields. Since there is little structure in the nuclear wave function with momentum components above 3 fm^{-1}, and higher momentum modes have sufficently high frequencies to be described adiabatically, we have truncated the expansion at $n_s=n_V=L/(2\text{ fm})$. This corresponds to a maximum physical momentum ≈ 3 fm^{-1}. This truncation is justified *a posteriori* because lower modes are also found to be essentially adiabatic. The length L must be sufficiently large to encompass the system with negligible edge effects. In our calculations, we used box sizes ranging from $L=16$ fm for light nuclei to $L=39$ fm for $A=20$.

The trial function Λ for nucleons in finite nuclei was chosen to be a product of an odd two-body correlation factor times a product of single-particle wave functions parametrized as follows:

$$\Lambda(x_1,x_2,\ldots,x_A)=\prod_{i<j}G(x_i-x_j)\prod_k F(x_k)\ , \tag{4.1}$$

where

$$G(x)=\tanh(bx) \tag{4.2}$$

and

$$F(x)=(1+e^{a(x-R)})^{-1}(1+e^{-a(x+R)})^{-1}\ . \tag{4.3}$$

Reasonable values for the parameters a, b, and R were selected on physical grounds and optimized by minimizing the variational energy with the static interactions.

Nuclear matter was calculated by enclosing A particles in a box of length L with periodic boundary conditions. For A greater than $\rho_0 L$, where ρ_0 is the saturation density, the ground state corresponds to uniform nuclear matter, and for A substantially less than $\rho_0 L$, nucleons coalesce into isolated nuclei. We have verified that the periodic solution at ρ_0 with $L=16$ fm is a valid approximation to nuclear matter by reproducing the same energy per nucleon as at $L=10$ fm. (See Fig. 7 in Appendix A.) With periodic boundary conditions, the trial function must also be periodic. Hence, we have used Eq. (4.1) with $F=1$ and

$$G(x)=\sin(\pi x/L)\ , \tag{4.4}$$

which corresponds precisely to a Fermi-gas Slater determinant.[5]

All Monte Carlo results in this section contain two distinct errors. Statistical errors arising from finite sample size are estimated as described in Appendix A and are denoted by error bars on the graphs. Systematic errors are introduced into all calculations by the use of a finite step size Δt. As explained and illustrated in Appendix A, all observables may be straightforwardly extrapolated to $\Delta t=0$. In the present section, the value of Δt will be specified for each figure and comparisons will be carried out at a fixed Δt. The essential results presented in this

section should not require any specialized knowledge of Monte Carlo technology, and further technical details are relegated to the appendices.

A. Energies

The binding energy is defined as the difference between the energy of A isolated, dressed nucleons, including the meson self-energy contributions, and the total energy of the interacting A-body system. In a practical calculation, it is then necessary to calculate separately the one-body and A-body systems.

In the static limit, the contribution of the static meson fields to the nucleon energy, Eq. (3.34), is 188.42 MeV for the parameters in Table I and with $L=16$ fm. Although it is artificial in a static potential theory to decompose the nucleon mass into a bare energy and a self-energy arising from meson fields, this static meson contribution sets the scale for interpreting self-energies in the field theory with dynamic mesons. The nucleon self-energies with $n_s=8$ or with $n_V=8$ using $\Delta t=10^{-4}$ MeV^{-1} are 192.3 ± 0.2 MeV or 191.1 ± 0.2 MeV, respectively. This is the first of many results in this section which show that the dynamic effect of meson fields on ground-state properties is small in this model. In comparison with the static theory, the nucleon self-energy in the dynamic theory with either scalar or vector mesons is shifted by only 2%. For our present purposes, as long as dynamic effects are small, it will suffice to consider the effects of scalar and vector dynamics separately.

The binding energy per nucleon in nuclear matter is shown in Fig. 2. The solid curve in the upper portion of the figure shows the mean-field result, Eq. (3.15). Recall that the parameters of the model were defined such that the saturation point of the mean-field theory, rather than that of the exact solution, corresponded to the physical value of the binding energy. Also shown is the conventional Hartree-Fock (HF) result, which is given by

$$\frac{E_{\rm HF}}{A}=\frac{\pi^2}{6}\frac{\rho^2}{M}+\frac{1}{2}\left[\frac{g_V^2}{m_V^2}(1-e_V)-\frac{g_s^2}{m_s^2}(1-e_s)\right]\rho\ , \tag{4.5a}$$

$$e_i\equiv\frac{m_i}{\pi\rho}\tan^{-1}\left[\frac{2\pi\rho}{m_i}\right]-\left[\frac{m_i}{2\pi\rho}\right]^2\ln\left[1+\left[\frac{2\pi\rho}{m_i}\right]^2\right]\ . \tag{4.5b}$$

Monte Carlo results are shown in the lower portion of Fig. 2. We regard the saturation curve for the static interaction extrapolated to $\Delta t=0$ using the method described in Appendix A as the exact nuclear matter solution for the static theory. Note that for $\rho>\rho_0$, the solution is uniform nuclear matter. Clustering begins below ρ_0, and in Fig. 2, the points at $\rho=0.25$ and 0.375 fm^{-1} correspond to essentially isolated nuclei with $A=4$ and 6, respectively.

Results for a finite Δt with dynamic scalar mesons and dynamic vector mesons are also shown in Fig. 2, as are the static calculations with the same Δt. These should be compared with each other, and not with the extrapolated

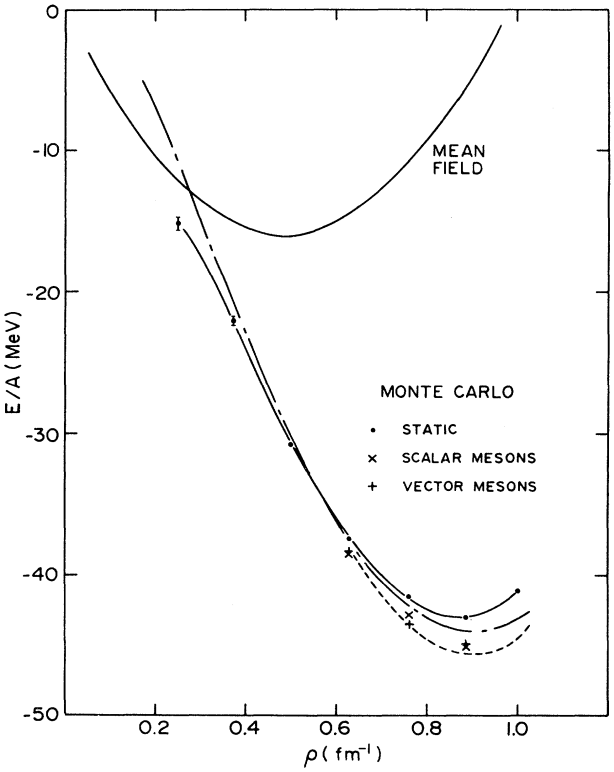

FIG. 2. Nuclear matter saturation curves. The energy per nucleon (negative of the binding energy) is plotted as a function of density for the mean field approximation (upper solid curve), Hartree-Fock approximation (dashed-dotted curve), and Monte Carlo calculations. The dots, × 's, and crosses denote calculations with the static potential, dynamic scalar modes, and dynamic vector modes, respectively, using a time step $\Delta t=0.001$ MeV^{-1}. Statistical errors are the size of the symbols unless shown explicitly, and the solid line connecting the Monte Carlo results is drawn to guide the eye. The dashed line shows the static potential saturation curve extrapolated to $\Delta t=0$. A box of length 16 fm with periodic boundary conditions was used with variable numbers of particles, and dynamic meson calculations used $n_s=8$ or $n_V=8$, corresponding to a maximum momentum of 3.14 fm^{-1}.

($\Delta t=0$) static curve. (The relatively small extrapolation correction indicates that this comparison at finite Δt will reflect the relevant qualitative effect of dynamic mesons.) As in the case of the nucleon self-energies, the effect of dynamic mesons is relatively small. Inclusion of vector or scalar mesons separately shifts the saturation density by the order of 5%, so the total effect is expected to be of the order of 10%. In contrast to the mean-field approximation, which yields only about one-third of the full binding energy at roughly one-half of the saturation density, the static approximation reproduces the saturation curve to within 10%.

Binding energies for a range of finite nuclei with the static interaction are shown in Fig. 3. The semiempirical mass formula in one dimension with no long-range forces or isospin contains only a volume term and surface term,

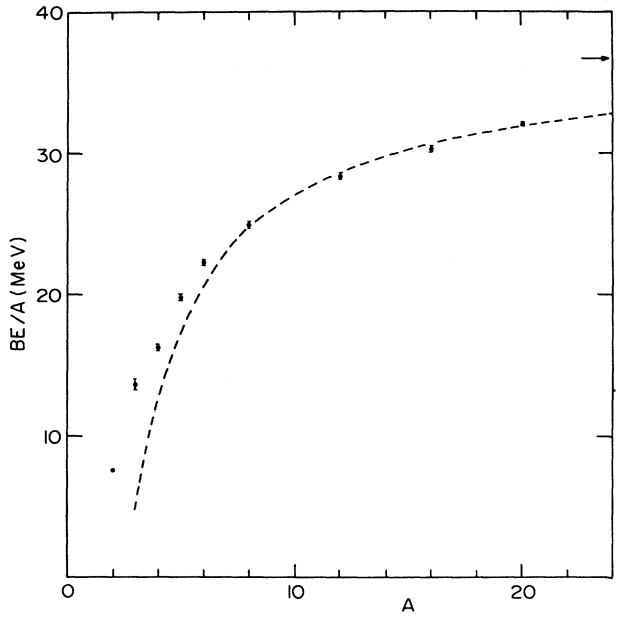

FIG. 3. Binding energy per nucleon of finite nuclei comprised of A nucleons bound by the static potential. Trial energies evaluated with $\Delta t=0.003$ MeV^{-1} are shown with statistical error bars. For $A<8$ the box length was 16 fm and for $A\geq 8$ the length was 32 fm. The dashed curve denotes the semiempirical mass formula with volume energy coefficient 36.7 MeV and surface energy coefficient 48.9 MeV. The arrow indicates the infinite nuclear matter limit.

$$\frac{E_B}{A}=a_V-2\frac{a_S}{A}\ . \tag{4.6}$$

A fit to the energies of the four largest nuclei using this mass formula yields the values $a_V=36.7$ MeV and $a_S=48.9$ MeV. That a_V and the nuclear matter binding energy for the same Δt, 37.1 ± 0.1 MeV, are nearly equal indicates saturation for heavy nuclei. The failure of Eq. (4.6) for light nuclei, however, suggests that saturation does not set in as early in this model as in real nuclei. (Note that the Pb nucleus, the paradigm for a heavy saturated nucleus, is only six nucleons thick measured through the center.)

The effect of dynamic mesons on the binding energies of finite nuclei is comparable to that observed in nuclear matter. Relative to the binding energy per particle of 28.3 ± 0.2 MeV in the $A=12$ nucleus obtained for the static potential, dynamical meson calculations with $n_s=8$ or $n_V=8$ yield 29.2 ± 0.2 or 28.6 ± 0.2 MeV, respectively, indicating a total shift due to mesons of the order of 5%.

B. Density distributions

To further explore the nuclear ground state in this theory, we have calculated one-body density distributions and two-body correlation functions. The nucleon-nucleon correlation function in nuclear matter is defined as

$$g(x)=\frac{1}{(A-1)\rho}\int dy\left\langle\Psi\left|\hat{\rho}\left[y+\frac{x}{2}\right]\hat{\rho}\left[y-\frac{x}{2}\right]-\delta(x)\hat{\rho}(y)\right|\Psi\right\rangle\Big/\langle\Psi\,|\,\Psi\rangle$$
$$=\frac{\left\langle\Psi\left|\sum_{i\neq j}\delta(\,|x_i-x_j|-x)\right|\Psi\right\rangle}{(A-1)\rho\langle\Psi\,|\,\Psi\rangle}\ , \tag{4.7}$$

with normalization such that g approaches unity at large x. In a practical Monte Carlo calculation, the x continuum is divided into discrete intervals, and the average of Eq. (4.7) is calculated for each interval using Eq. (2.10). In the results presented here, the average value for each interval is plotted at the midpoint with statistical errors, and the interval size is obvious from the spacing of data points.

The nucleon-nucleon correlation function for the static interaction at $\rho=0.75$ fm^{-1} (near saturation density) is shown by the data points in Fig. 4. For comparison, the correlation function for a Fermi-gas Slater determinant, calculated using the same discrete intervals, is denoted by a solid curve. Qualitatively, the dynamical correlations included in the exact result beyond those imposed by antisymmetry display the expected physical behavior. The repulsive core inside 0.5 fm decreases the probability at short range relative to that of the Fermi gas, and in the region of maximum attraction around 1 fm the probability is correspondingly enhanced. At larger distances, the "healing" of the two-body correlation function arising

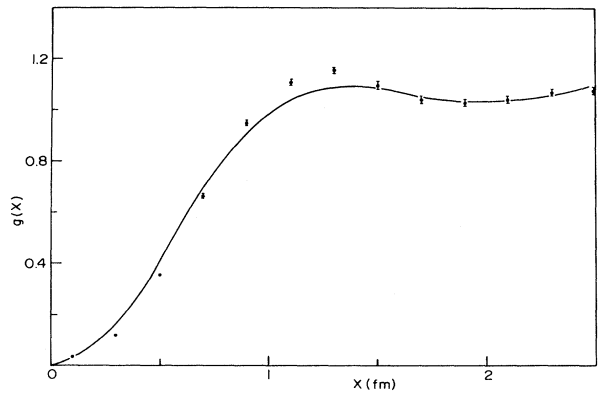

FIG. 4. Nucleon-nucleon correlation function $g(x)$ in nuclear matter. Monte Carlo results at $\rho=0.75$ fm with $\Delta t=0.0005$ MeV^{-1} for the static interactions are shown in the center of each averaging interval by statistical error bars. For comparison, the values of the correlation function for a Fermi-gas Slater determinant calculated in the same averaging intervals are connected by the smooth solid curve.

from Pauli blocking of all available scattering states is evident from the agreement between the exact and Fermi-gas correlation functions.

Quantitatively, the dynamical correlations in our model are significantly weaker than those arising in three-dimensional calculations with phenomenological potentials. A manifestation of this weak core is the relatively minor suppression of $g(x)$ inside the core radius. In comparison, a potential like the Reid soft-core yields a $g(x)$ which remains nearly zero throughout the core region.

The inclusion of dynamic vector or scalar mesons does not yield results for $g(x)$ statistically different from those displayed in Fig. 3. Hence, any differences must be less than one percent. Given the facts that energies calculated with static and dynamic interactions differ on the order of 10% and that the interaction only contributes at most a 10% deviation in $g(x)$ relative to the Fermi gas result, it is not surprising that the final sensitivity of $g(x)$ to dynamical mesons is below one percent.

The meson correlation function may be defined analogously to Eq. (4.7) and evaluated in momentum space. Using the notation of Eq. (3.19),

$$\tilde{G}_k=\sqrt{2/L}\int_0^L dx\cos\left[\frac{2\pi k}{L}x\right]\left[\frac{1}{L}\int dy\frac{\langle\Psi|\varphi(y+x/2)\varphi(y-x/2)|\Psi\rangle}{\langle\Psi|\Psi\rangle}\right]$$
$$=\frac{1}{\sqrt{2L}}\langle\varphi_k^2+\tilde{\varphi}_k^2\rangle\ . \tag{4.8}$$

Since $\{\varphi_k\}$ are the coordinates describing the fields, $\langle\varphi_k^2\rangle$ may be straightforwardly evaluated in the Monte Carlo calculation using Eq. (2.10). For comparison, the expectation value of φ_k^2 for the static modes is obtained directly from the displaced harmonic oscillator wave function for the meson field, Eq. (3.38), with the result

$$\langle\varphi_k^2\rangle_{\text{static}}=\chi_k^2+\frac{1}{2\omega_k}\ . \tag{4.9}$$

A Monte Carlo calculation with $n_s=8$ at $\rho=0.875$ fm^{-1} yielded values for $\tilde{G}_k$ which were identical to the static result for each mode to within statistical errors of one percent. Repetition of the calculation with a much smaller scalar meson mass, $m_s=14$ MeV, yielded the same result. Thus, with respect to equal-time correlation functions, the mesons are essentially static.

The one-body density distributions for finite nuclei, like the nucleon-nucleon correlation function, are calculated by evaluating the one-body density over a finite interval using Eq. (2.10). In order for the perturbation expression (2.10) for the density to be accurate, the trial density itself must yield a reasonable approximation. In Appendix A we demonstrate that our trial functions and the perturbation expression are adequate, by showing that the corrected density is independent of the trial function.

Density distributions for finite nuclei from $A=4$ to $A=20$ using the static interaction are shown in Fig. 5. For the lightest nuclei, the averaging intervals are sufficiently small that the quantum density fluctuations and surface shape are accurately portrayed. For the largest nuclei, however, much of this structure is averaged out. For example, each point in the $A=20$ system corresponds to the average of three or four points in the $A=4$ system, and one may observe directly in the figure that most of the structure for $A=4$ would be removed if each group of three or four points were replaced by its average. Quantum density fluctuations for a similar one-dimensional system are studied with much higher resolution in Ref. 5.

The essential physical effect displayed in Fig. 5 is the unusually slow saturation of the interior density with increasing A. In real nuclei, in calculations of finite nuclei

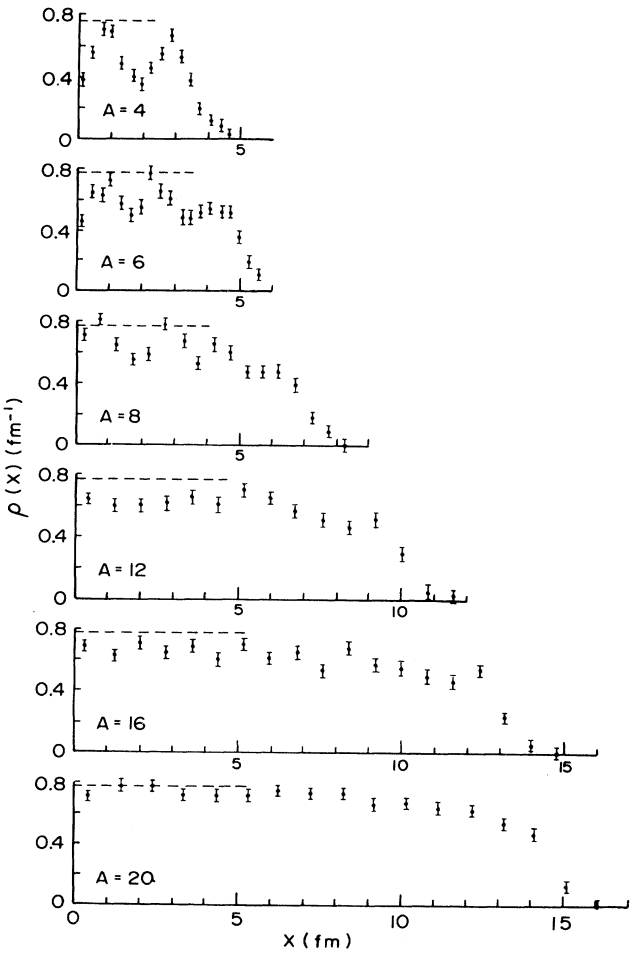

FIG. 5. Density distribution for finite nuclei. Monte Carlo results with statistical errors using $\Delta t=0.003$ MeV^{-1} are shown for the average density in each of 20 spatial bins as described in the text. The saturation density for nuclear matter for the same Δt is $\rho=0.77$ fm^{-1} and is indicated by the dashed line.

in three dimensions with realistic interactions, and in the one-dimensional model of Ref. 5, the average interior density of light nuclei is very close to that of nuclear matter. In contrast, the average interior density of nuclei from $A=4$ to $A=8$ in Fig. 5 differs from the nuclear matter values indicated by the dashed line by from 30% to 15%. Only in the heaviest nuclei, such as $A=20$, shown at the bottom of the figure, does the interior density approach that of nuclear matter. Thus, in addition to the slow onset of liquid-drop behavior with increasing A discussed in connection with Fig. 3, the slow approach to nuclear density shown in Fig. 5 provides independent evidence of the unusually slow saturation arising in the present model.

V. SUMMARY AND CONCLUSIONS

In this work, we have investigated a nonrelativistic theory of nucleons coupled to vector and scalar mesons. By restricting the model to one spatial dimension, it has been possible to exploit fermion Monte Carlo techniques to compare exact solutions to the theory including dynamic mesons with exact solutions to the corresponding potential theory in which all meson modes are static.

Our main physical result is that dynamic mesons introduce small changes relative to the static potential theory for the observables we have investigated. For this model, at least, we have thus justified the conventional approach to nuclear many-body theory, in which a nucleus is described in first approximation in terms of nucleon degrees of freedom interacting via static potentials, and the dynamic effects of subnuclear degrees of freedom are treated as small perturbations. The physical origin of this nearly adiabatic behavior is evident from the Born-Oppenheimer approximation to the Hamiltonian, Eq. (3.37), provided by the trial function, Eq. (3.38). To the extent to which the nucleon motion is slow compared to the meson frequencies ω_n and Ω_n, the displaced oscillator wave function for the meson fields accurately describes the essentially instantaneous adjustment of the mesons.

In contrast to the accuracy of the static potential approximation, we have shown that the mean-field approximation does not describe the nuclear matter saturation density and energy. A particularly striking feature of the mean-field theory, when viewed from the context of the present work, is that it involves precisely the $n=0$ modes which decouple from the dynamic meson and nuclear degrees of freedom in Eq. (3.37). To the extent to which saturation arises from strong repulsive short-range interactions corresponding to multiple exchanges of vector mesons, it is clear that this physical effect is totally ignored in the mean-field approximation but sensibly approximated by the exact static potential approximation, or even in the conventional HF approximation.

Despite the obvious physical limitations of one-dimensional models, it is reasonable to expect these conclusions concerning the static and mean-field approximations to apply as well to three dimensions. Repulsive short-range interactions are even more important in producing saturation in three dimensions than in one dimension, since the kinetic energy alone can saturate a one-dimensional system with attractive interactions, but not a three-dimensional system. The arguments concerning the decoupling of dynamic modes from the $n=0$ mean-field terms and the Born-Oppenheimer justification of the static potential limit are, of course, independent of dimension.

Relativistic effects (which have been neglected here) may also play a significant role in the saturation in three dimensions. In particular, maintaining the Lorentz scalar and vector character of the meson potentials and nucleon source terms leads to additional density dependence in the nucleon-nucleon interaction.[1] Thus, the conclusions concerning the mean-field approximation obtained in the nonrelativistic limit may not apply to a relativistic treatment of our model.

One avoidable pathology of the model calculations reported in this work is the slow saturation of the density and binding energy with the nucleon number A. This slow saturation arises from the long range of the potential in Fig. 1 resulting from setting the scalar meson mass equal to that of the pion and from the fact that the interaction parameters were determined by mean field rather than exact nuclear matter properties. The use of the light scalar meson mass has the pedagogical advantage of emphasizing rather than obscuring any effects of meson dynamics. In realistic calculations of the nucleon-nucleon potential, one-pion exchange gives an essentially negligible contribution to the intermediate range attraction, which is dominated by two-pion exchange. Thus, the range of the attractive nuclear force is characterized by twice the pion mass and phenomenological potentials fit to scattering data are of considerably shorter range than that of Fig. 1. From Fig. 2, it is evident that if the potential parameters in our model were readjusted so that the exact Monte Carlo calculation saturated at $E/A \sim 16$ MeV and $k_F \sim 1.3$ fm^{-1}, the static potential would acquire a substantially stronger vector meson repulsive core. Decreasing the range of the attraction and increasing the core repulsion would yield a static potential more similar to the model interaction of Ref. 5. The latter interaction was defined to reproduce appropriate dimensionless ratios characterizing realistic nuclear interactions in three dimensions, and produced saturation with A comparable to that observed in real nuclei. Thus, we believe the slow saturation of the model used in the present work is an artifact of the parameter values selected for this initial exploration and does not materially alter the physical conclusions we have drawn.

From a technical perspective, this work represents a first step in the development of exact stochastic techniques for dealing with non-nucleon degrees of freedom in nuclei. Motivated by the success of using trial functions in quantum many-body systems to guide Monte Carlo random walks, we have demonstrated that a trial function is also useful in guiding the stochastic evolution of meson fields. The use of a displaced oscillator wave function for the fields had two substantial benefits. Since the Born-Oppenheimer approximation is quite accurate, the random walk for the meson degrees of freedom is biased by an excellent approximation to the exact solution, requiring the Monte Carlo calculation to account for only very small dynamic departure from adiabaticity. Second, truncation of the expansion in meson modes was facilitated by the

possibility of summing the oscillator contributions for all n analytically via Eq. (3.35), and then including the difference between dynamic evolution and the oscillator approximation for a finite number of low-momentum modes. This treatment of the meson degrees of freedom is not restricted to one dimension and should be valuable in realistic applications in three dimensions.

Two generalizations of the present work offer fruitful avenues for future investigations. For a one-dimensional system, it is possible to treat the full relativistic Hamiltonian, Eq. (3.9). The meson field equations have an analogous Fourier expansion, with source terms which contain both the baryon ($\psi^\dagger\psi$) and scalar ($\bar{\psi}\psi$) density. The nonrelativistic Schrödinger equations with continuum x may be replaced by the Dirac equation on a discrete spatial lattice, and the number of dynamical fermions equals the number of mesh points plus A. In this way, it will be possible to assess the effect of relativistic kinematics and the role of polarizations of the Dirac sea. For spin-isospin independent coupling, it is also practical to solve the α particle with the present nonrelativistic Hamiltonian in three dimensions, providing a more definitive test of the role of meson dynamics.

Extension of the methods used in this work to realistic nuclei in three dimensions still poses substantial difficulties. The addition of spin-isospin dependent interactions to study pions or treatment of nuclei in three dimensions with $A>4$ gives rise to formidable practical problems arising from nearly cancelling positive and negative contributions to Monte Carlo estimates of observables. These further generalizations may be treated in principle either using transient estimates[11] or by reformulating the problem on a discrete spatial mesh.[17] Since both approaches lie at or beyond the limits of currently available computer facilities, the development of more powerful stochastic techniques for many-fermion problems remains a major conceptual challenge in this field.

This work was supported in part by the National Science Foundation (U.S. Grants Nos. PHY77-27084, PHY79-23638, PHY81-07395, and PHY82-07332), and by the U.S. Department of Energy (Grant No. DE-AC02-76ER03069). J. W. Negele and Brian Serot gratefully acknowledge fellowship support by the John Simon Guggenheim Memorial Foundation and the Alfred P. Sloan Research Foundation, respectively.

APPENDIX A: COMPUTATIONAL TECHNIQUES

One of the most important features of our numerical method is the use of a finite time step Δt. This has several implications which must be carefully considered in actually performing calculations and which constrain Δt to be neither too small nor too large. Some of these are discussed in this appendix.

Our method becomes exact in the limit $\Delta t \to 0$, which is, of course, impossible to reach in practice. A practical lower bound to Δt is given by the rate at which configurations in the ensemble explore phase space. Once the ensemble of configurations has been relaxed (i.e., by evolving it for some time), the precision of the energy estimators is improved by averaging their values at many different subsequent times. For such an average to be meaningful and for its variance to be estimated accurately, statistically independent values must be averaged. However, when Δt is very small, Eq. (2.9) shows that the ensemble evolves very slowly ($q \approx q'$), and successive values of the energy estimators are highly correlated. For example, Fig. 6 shows the autocorrelation function of the energy estimator $E(t)$ [given by (2.6)] for a representative system with several different Δt. This quantity is defined as

$$c(\tau)=\frac{\langle [E(t+\tau)-\bar{E}][E(t)-\bar{E}]\rangle}{\langle [E(t)-\bar{E}]^2\rangle}\ , \tag{A1}$$

where $\langle\ \rangle$ denotes time average and $\bar{E}=\langle E(t)\rangle$ is the average energy. When Δt is small, c is nonzero for many time steps, so that energy values must be accumulated infrequently, resulting in increased computational effort for a given precision.

A practical upper bound on Δt is set by the accuracy with which (2.9) approximates (2.7). This clearly requires that the average nucleon "step" in the diffusion process, $(\Delta t/M)^{1/2}$, be small compared to the other characteristic length scales. If we take the latter to be 0.2 fm, we find $\Delta t \lesssim 0.001\ \text{MeV}^{-1}$. However, when there are dynamic meson modes present, an even shorter time step is required to evolve the high frequency modes ($\Omega_n \gtrsim 783$ MeV implies $\Delta T \lesssim 10^{-4}\ \text{MeV}^{-1}$). This can be at least partially alleviated by using a more accurate treatment of the meson propagation over Δt. Consider a single scalar meson mode φ with frequency ω, in the presence of static nucleons giving a classical solution χ as in (3.30a). In this case, with a trial function of the form (3.29), (2.7) gives the evolution as (putting $E_N=0$)

$$\frac{\partial G}{\partial t}(\varphi,t)=\frac{1}{2}\frac{\partial^2 G}{\partial \varphi^2}+\omega\frac{\partial}{\partial\varphi}[(\varphi-\chi)G]-\frac{\omega}{2}G=0\ . \tag{A2}$$

This Fokker-Planck equation can be solved by the (unnormalized) kernel

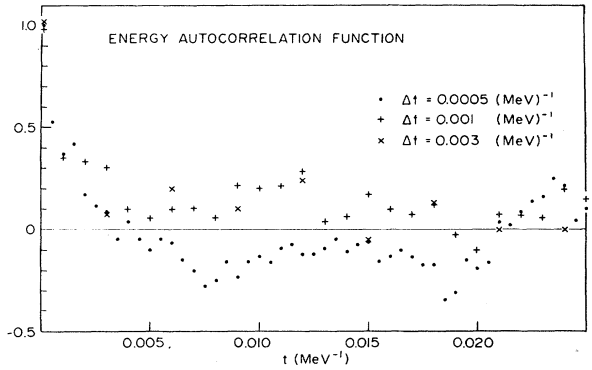

FIG. 6. Energy autocorrelation function, Eq. (A1), as a function of time for a twelve-particle system with $n_s=8$.

$$K(\varphi,\varphi';\Delta t)=\exp\left\{-\frac{[\varphi-\varphi' e^{-\omega\Delta t}+(1-e^{-\omega\Delta t})\chi]^2}{(1-e^{-2\omega\Delta t})/\omega}\right\}, \tag{A3}$$

which has the expected limits

$$\lim_{\Delta t\to 0} K(\varphi,\varphi';\Delta t)=\exp\left\{-\frac{[\varphi-\varphi'+\omega\Delta t(\varphi'-\chi)]^2}{2\Delta t}\right\}, \tag{A4a}$$

$$\lim_{\Delta t\to\infty} K(\varphi,\varphi';\Delta t)=\exp[-\omega(\varphi-\chi)^2]\ . \tag{A4b}$$

Hence, by suitably renormalizing the drift and dispersion terms in the Gaussian kernel for the evolution of the field variables, the analytically known properties of the harmonic-oscillator Hamiltonian can be exploited to achieve a more accurate evolution of the high-frequency modes for a finite time step.

Our calculations typically used an ensemble of 100 configurations evolved over a time 1.5 MeV^{-1} after relaxation (requiring typically $T=0.3$ MeV^{-1}). Sampling frequencies were determined in each case by analyzing the energy autocorrelation function, as discussed above. These were typically every five time steps. The extrapolation of the Monte Carlo results to the $\Delta t=0$ limit is illustrated in Fig. 7. Note that the trial and normalization estimators agree within the statistical errors. We have also verified, in selected cases, that our trial functions Φ are adequate, in that the calculated energies and densities are independent of the precise trial function chosen (see Fig. 8).

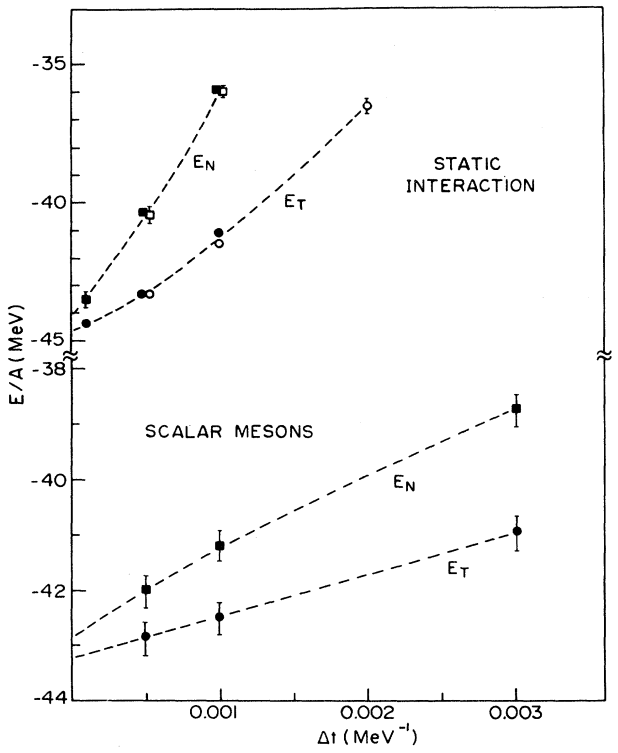

FIG. 7. Calculated energy per particle in nuclear matter as a function of time step Δt. The square and round symbols denote normalization and trial energies [Eqs. (2.2) and (2.6)], respectively, the statistical errors are the size of the symbols unless indicated by error bars, and the dashed curves are to guide the eye. The upper portion shows the energy per nucleon with the static interaction at $\rho=1$ fm^{-1} calculated in a box of length 10 fm (open symbols) and a box of length 16 fm (filled symbols). The lower portion shows the energy per nucleon including scalar mesons with $n_s=8$ in a box of length 16 fm at $\rho=0.75$ fm^{-1}.

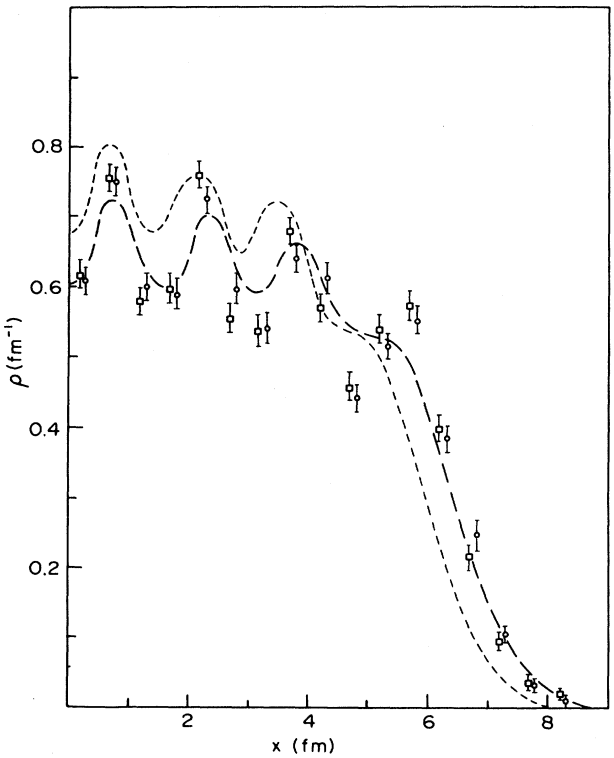

FIG. 8. Density distributions for $A=8$ nucleons demonstrating that different trial functions yield consistent ground state densities. Density distributions for the trial function given in Eqs. (4.1)—(4.3) with $a=1$ fm^{-1}, $b=0.5$ fm^{-1}, and $R=4$ or 5 fm are denoted by the short or long dashed curves, respectively. Monte Carlo results for the ground-state density using the perturbative expression (2.10) are given by the square and circular data points for calculations using the $R=4$ and $R=5$ trial functions, respectively. Despite the substantial difference in trial densities, the Monte Carlo densities agree within statistical errors denoted by the error bars.

APPENDIX B: VECTOR MESON COUPLING TO THE BARYON CURRENT

As discussed in Sec. III, the nonrelativistic model used in our investigation was defined by eliminating the coupling

$$\mathscr{H}_I\equiv g_V\psi^\dagger\alpha\psi V \tag{B1}$$

from the interaction Hamiltonian density in Eq. (3.9d). Since the matrix α mixes upper and lower components of

the Dirac spinors ψ, this interaction term is (at least) of order $(1/M)$ and thus represents relativistic corrections. These corrections are, of course, necessary to maintain the global U(1) gauge invariance of the Lagrangian (3.1) that ensures conservation of the baryon current. Here we describe how these corrections may be included in the Monte Carlo analysis.

Note first that by combining $\mathscr{H}_1$ with the free Dirac Hamiltonian density (3.9a), we find

$$\mathscr{H}_F^0+\mathscr{H}_1=\psi^\dagger\left[\alpha\left[-i\frac{\partial}{\partial x}-g_V V\right]+\beta M\right]\psi\,. \tag{B2}$$

This illustrates that the coupling of the baryons to V is identical to their coupling to the (spatial) vector potential A in spinor QED. Thus, by performing the standard Foldy-Wouthuysen reduction,[15,18] we may rewrite Eq. (A2) in terms of nonrelativistic Schrödinger fields to any desired order in $(1/M)$. We will work consistently to $O(1/M)$ and find

$$\mathscr{H}_F^0+\mathscr{H}_1\simeq\psi_{\rm NR}^\dagger\left[M+\frac{p^2}{2M}\right]\psi_{\rm NR}-\frac{g_V}{2M}\psi_{\rm NR}^\dagger(pV+Vp)\psi_{\rm NR}+\frac{g_V^2}{2M}V^2\psi_{\rm NR}^\dagger\psi_{\rm NR}+O(1/M^2)\,, \tag{B3}$$

where $p=-i\partial/\partial x$. Corrections to the interaction terms involving the electric field E [see Eq. (3.9d)] enter at $O(1/M^2)$ and so may be neglected in this approximation.

The first term in Eq. (B3) gives the free Schrödinger Hamiltonian density, and we may write the (approximate) interaction terms as

$$H_1\equiv\int dx\,\mathscr{H}_1(x)\simeq i\frac{g_V}{2M}\sum_{i=1}^{A}\left[2V(x_i)\frac{\partial}{\partial x_i}+\left[\frac{\partial V}{\partial x}\right]_{x=x_i}\right]+\frac{g_V^2}{2M}\sum_{i=1}^{A}V^2(x_i)+O(1/M^2)\,, \tag{B4}$$

where we have gone to first quantization for the nucleons and partially integrated the momentum operator, dropping the surface terms. Note that H_1 does not contribute to the mean-field energy in nuclear matter, because $V\equiv 0$ by reflection invariance. Thus Eq. (3.15) and the subsequent discussion are valid even when H_1 is retained in the model Hamiltonian.

We now rewrite H_1 using Fourier components for the field V, which is considered the conjugate momentum to the electric field E, as in Sec. III. Thus,

$$V(x)=-i\frac{\delta}{\delta E(x)}=-i\sqrt{2L}\left\{\frac{\partial}{\partial E_0}+\sum_{n=1}^{\infty}\left[\sin\left[\frac{2\pi n}{L}x\right]\frac{\partial}{\partial E_n}+\cos\left[\frac{2\pi n}{L}x\right]\frac{\partial}{\partial\tilde{E}_n}\right]\right\}, \tag{B5}$$

which leads to

$$\begin{aligned}H_1\simeq&\frac{g_V}{m_V M}\sqrt{2/L}\sum_{i=1}^{A}\sum_{n=1}^{\infty}\sin\left[\frac{2\pi n}{L}x_i\right]\frac{\partial}{\partial\hat{E}_n}\frac{\partial}{\partial x_i}+\frac{g_V}{2m_V M}\sum_{i=1}^{A}\sum_{n=1}^{\infty}\frac{\partial\rho_n}{\partial x_i}\frac{\partial}{\partial\hat{E}_n}\\&+\frac{g_V}{m_V M}\sqrt{2/L}\frac{\partial}{\partial\hat{E}_0}\sum_{i=1}^{A}\frac{\partial}{\partial x_i}-\frac{g_V^2}{m_V^2 M}\frac{1}{L}\sum_{i=1}^{A}\sum_{n,n'=1}^{\infty}B_{nn'}(x_i)\frac{\partial}{\partial\hat{E}_n}\frac{\partial}{\partial\hat{E}_{n'}}\\&-\frac{g_V^2}{m_V^2 M}\sqrt{2/L}\frac{\partial}{\partial\hat{E}_0}\sum_{n=1}^{\infty}\rho_n\frac{\partial}{\partial\hat{E}_n}-\frac{\partial}{\partial\hat{E}_0^2}+\tfrac{1}{4}m_V^2\hat{E}_0^2+\frac{1}{2}\frac{g_V^2}{m_V^2}\frac{A^2}{L}-\frac{g_V^2}{m_V^2 M}\frac{A}{L}\frac{\partial^2}{\partial\hat{E}_0^2}+O(1/M^2)\,.\end{aligned} \tag{B6}$$

Here we indicate explicitly the sums over Fourier sine components only, and the field variables $\hat{E}_n$ are defined in Eq. (3.22c). The matrix B is given by

$$B_{nn'}(x_i)=\begin{pmatrix}\sin\left[\frac{2\pi n}{L}x_i\right]\sin\left[\frac{2\pi n'}{L}x_i\right] & \sin\left[\frac{2\pi n}{L}x_i\right]\cos\left[\frac{2\pi n'}{L}x_i\right]\\ \cos\left[\frac{2\pi n}{L}x_i\right]\sin\left[\frac{2\pi n'}{L}x_i\right] & \cos\left[\frac{2\pi n}{L}x_i\right]\cos\left[\frac{2\pi n'}{L}x_i\right]\end{pmatrix}. \tag{B7}$$

The first three terms in Eq. (B6) originate from the coupling of the nucleon current to V and introduce mixed derivatives $\partial^2/\partial\hat{E}_n\partial x_i$. The remaining terms come from the V^2 ("seagull") piece in H_1 and introduce off-diagonal derivatives $\partial^2/\partial\hat{E}_n\partial\hat{E}_{n'}$. Note also that the $n=0$ modes are now coupled to the $n\neq 0$ modes and hence we have included the relevant part of the $n=0$ Hamiltonian H_0 [cf. Eq. (3.25)].

Because of the new cross terms, H_1 is not of the form described in Sec. II. Schematically, we can represent the full Hamiltonian as

$$H=\sum_{q,q'}T_{qq'}\frac{\partial}{\partial q}\frac{\partial}{\partial q'}+\sum_q V\left[q,\frac{\partial}{\partial q}\right], \tag{B8}$$

where q stands either for field variables or nucleon coordinates. [The form studied in Sec. II is obtained if

$T_{qq'} \propto \delta_{qq'}$ and V depends only on coordinates: $V = V(q)$.] Here V incorporates the first three terms in Eq. (B6), while all remaining terms are included in $T_{qq'}$. The new form of the Hamiltonian requires three modifications in implementing the Monte Carlo procedure, all of which may be carried out straightforwardly in practical applications.

First, in determining the trial meson wave function [Eq. (3.38)], one must invert and calculate the determinant of the matrix T. This may be easily done to $O(1/M)$, which is sufficient, since the reduction procedure leading to Eq. (B3) already omits corrections of $O(1/M^2)$ in the diagonal elements of T. Second, in evaluating the drift terms in the evolution operator [see Eq. (2.8)], one must include the momentum-dependent terms appearing in the potential $V(q,\partial/\partial q)$. This is also straightforward. Finally, to write the Hamiltonian with a finite number of vector meson modes, one must include the corrections of order $(1/M)$ to the static nucleon-nucleon potential (3.35). The first three terms in Eq. (B6) lead to a "recoil correction" of the form

$$V_{\mathrm{NN}}^{\mathrm{recoil}}(x_i,x_j) = \frac{g_V^2}{m_V^2}\left\{\frac{1}{2M}\frac{\partial}{\partial x_i}, \left[\frac{1}{2M}\frac{\partial}{\partial x_j}, \delta(x_i - x_j)\right]\right\}, \tag{B9}$$

where $\{a,b\} \equiv ab + ba$. There will also be modifications coming from the "seagull" vertex $\propto V^2$. These may be calculated by evaluating the energy from the remaining terms in Eq. (B6) in the limit of fixed baryons and then constructing a modified coordinate-space potential as in Sec. III. One may then include these corrections in the static Hamiltonian (3.36) and, as discussed in Sec. III, replace the desired number of dynamic modes using the expressions in Eq. (B6). Note that since (B9) is a "quasilocal" contact interaction, it can be used in the periodic system without worrying about images. In addition, since the corrections (B6) are already of order $(1/M)$ and dynamic effects of the vector meson are small, it may be possible to include these effects using the "static" potentials alone.

[1] J. D. Walecka, Ann. Phys. (N.Y.) 83, 491 (1971); S. A. Chin and J. D. Walecka, Phys. Lett. 52B, 24 (1974); S. A. Chin, Ann. Phys. (N.Y.) 108, 403 (1977).

[2] F. Lenz, E. Moniz, and K. Yazaki (unpublished); C. Horowitz, E. Moniz, and J. W. Negele (unpublished).

[3] Y. Alhassid, K. Chow, S. E. Koonin, K. Langanke, and G. Maddison (unpublished).

[4] S. E. Koonin, in *Nuclear Theory 1981,* edited by G. F. Bertsch (World Scientific, Singapore, 1981).

[5] J. W. Negele, in *Proceedings of the International Symposium on Time-Dependent Hartree-Fock and Beyond,* Lecture Notes in Physics 171, edited by K. Goeke and P. G. Reinhardt (Springer, New York, 1982).

[6] S. A. Chin, J. W. Negele, and S. E. Koonin (unpublished).

[7] M. H. Kalos, Phys. Rev. 128, 1791 (1962); J. Comput. Phys. 1, 257 (1966); Phys. Rev. A 2, 250 (1970); D. M. Ceperley and M. H. Kalos, in *Monte Carlo Methods in Statistical Mechanics,* edited by K. Binder (Springer, New York, 1979).

[8] N. Metropolis, A. Rosenbluth, M. Rosenbluth, A. Teller, and E. Teller, J. Chem. Phys. 21, 1087 (1953).

[9] M. H. Kalos, D. Levesque, and L. Verlet, Phys. Rev. A 9, 2178 (1979); P. A. Whitlock, M. H. Kalos, G. V. Chester, and D. M. Ceperley, Phys. Rev. B 19, 5598 (1979); M. H. Kalos, M. A. Lee, P. A. Whitlock, and G. V. Chester, *ibid.* 24, 115 (1981).

[10] J. B. Anderson, J. Chem. Phys. 63, 1499 (1975); 65, 4121 (1976); 73, 3897 (1980); 74, 6307 (1981); J. W. Moskowitz, K. E. Schmidt, M. A. Lee, and M. H. Kalos, J. Chem. Phys. 77, 349 (1982); P. J. Reynolds, D. M. Ceperley, B. J. Alder, and W. A. Lester, J. Chem. Phys. 77, 5593 (1982).

[11] D. M. Ceperley and B. J. Alder, Phys. Rev. Lett. 45, 566 (1980).

[12] D. M. Ceperley and B. J. Alder, Physica B&C 107, 875 (1981).

[13] J. G. Zabolitzky and M. H. Kalos, Nucl. Phys. A356, 114 (1981).

[14] C. J. Horowitz and B. D. Serot, Nucl. Phys. A368, 503 (1981).

[15] J. D. Bjorken and S. D. Drell, *Relativistic Quantum Mechanics* (McGraw-Hill, New York, 1964).

[16] Relativistic corrections to this result are of order $g_s\rho^3/m_s^2M^2$.

[17] S. E. Koonin, G. Sugiyama, and H. Friedrich, in *Proceedings of the International Symposium on Time-Dependent Hartree-Fock and Beyond,* Lecture Notes in Physics 171, Ref. 5, p. 214.

[18] L. L. Foldy and S. A. Wouthuysen, Phys. Rev. 78, 29 (1950).